

³ A. Pais and R. Serber, Phys. Rev. **99**, 1551 (1955).

⁴ O. Kofoed-Hansen, Phil. Mag. **42**, 1411 (1951).

⁵ J. Grussard, *et al.*, Nuovo Cimento **3**, 731 (1956).

⁶ G. Gosta and N. Dellaporta, Nuovo Cimento **2**, 519 (1955).

⁷ K. Iwata, *et al.*, Progr. Theor. Phys. **13**, 19 (1955).

Translated by C. R. Lubitz

107

Measurement of the Lifetimes of K -Mesons

M.IA. BALATS, P.I. LEBEDEV AND I.U.V. OBUKHOV

(Submitted to JETP editor June 7, 1956)

J. Exptl. Theoret. Phys. (U.S.S.R.) **31**, 531-533

(September, 1956)

THE measurement of the mean life of charged K -mesons from cosmic radiation has been carried out at sea level, using scintillation counters and a high-speed oscillograph¹. A charged unstable particle formed in a slab of lead A (Fig. 1) passed through counters C_1 and C_2 , and reached counter C_1 inside which was a brass absorber (10 gm/cm^2). Counters C_3 and C_3' then registered the decay

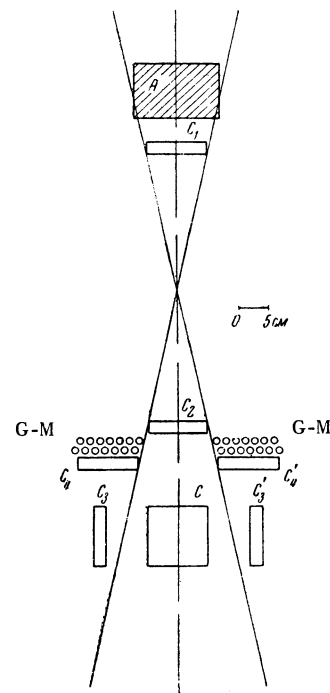


FIG. 1. Schematic diagram of set-up.

products of the particles which came to rest in C . The data on the liquid scintillation counters are collected below in a Table.

TABLE

Counter	Area cm ²	Thickness, cm	Solvent	Conc. of Terphenyl, g/l	Amount of FEU-19
C_1, C_2, C_3, C_3'	10×20	2	Toulene	3.5	1
C_4, C_4'	10×26	2	Benzene	1.4	2
C	10×20	10	Benzene	0.9	1

Pulses from the photomultipliers of the counters C_1, C_2, C_3 and C_3' were amplified, time-formed and fed to a coincidence counter². The amplifier band width was 210 mc , the amplification factor ~ 6 . In channels C_1 and C_2 pulses of length $4 \times 10^{-8} \text{ sec}$ were formed, in channels C_3 and C_3' , of length $6 \times 10^{-9} \text{ sec}$. The resolution curve of the coincidence circuit is given in Fig. 2. Triple coincidences $C_1 + C_2 + C_3$ or $C_1 + C_2 + C_3'$ triggered the oscilloscope and pulses coming from counter C were fed to the input of the vertical deflection amplifier. They were then photographed

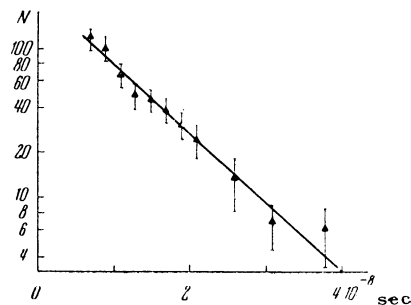


FIG. 2. Resolution curve for triple coincidences $C_1 + C_2 + C_3$.

on the oscilloscope screen. The duration of the sweep was 1.3×10^{-7} sec, and the minimum rise in the amplifier 2.5×10^{-9} sec. The precision of measuring the time between impulses was determined basically by the time dispersion of the photomultiplier belonging to counter C . To reduce this dispersion, we used a specially selected multiplier, type FEU-19. The exposed central part of the photocathode measured 5×12 mm, and the overall voltage was 4500 v.

The experimental error, connected with the time dispersion of a given FEU-19 tube, did not exceed 1.6×10^{-9} sec. In the photomultiplier there sometimes occurred a secondary spurious impulse following the basic impulse, but not connected with the passage of a particle through C . Such cases could imitate the decay of a K -meson when the set-up was triggered by shower particles. In view of this, it was necessary to reduce to a minimum the number of times the apparatus was triggered by showers.

In the first phase of this work, this was accomplished by including C_4 and C'_4 in anticoincidence with $C_1 + C_2 + C_3$ or $C_1 + C_2 + C'_3$. The efficiency of this method was 96%. The presence of a group of Geiger-Muller counters covering C_4 and C'_4 further reduced the number of times the system was triggered by showers. It is necessary to note that such a system excludes K -mesons accompanied by wide showers. Later on, the anticoincidence counters were replaced by a system of delayed coincidences, by introducing into channels C_1 and C_2 additional delay cables (1.4×10^{-8} sec).

From the resolution curve of Fig. 2 it can be seen that the probability of triggering the system by the simultaneous passage of particles through C_1, C_2, C_3 (C'_3) did not exceed 0.02.

In order to take account of the secondary photomultiplier impulses, and the time displacement between pulses which resulted from the different flight times of two related particles, we measured the distribution of time intervals between pulses in counter C . In phase I of the work, this was done by including C_4 and C'_4 in anticoincidence, while in phase II, we disconnected the additional delay cables. In such control investigations the number of delays in counter C was negligibly small. The results of these control experiments were included in the interpretation of the results.

The smallest energy of μ -meson decay which could also trigger the set-up was 25 mev. Therefore, we excluded cases of $\pi \rightarrow \mu + \nu$. The $\mu \rightarrow e$

$+ 2\nu$ decay could trigger the set-up, but in view of the fact that the resolution of the coincidence circuit was 4×10^{-8} sec, the probability of such an event was sufficiently small.

From among a total of 1600 cases, 64 were observed with a decay in an interval $10^{-8} - 4 \times 10^{-8}$ sec. The integral distribution of decay times is

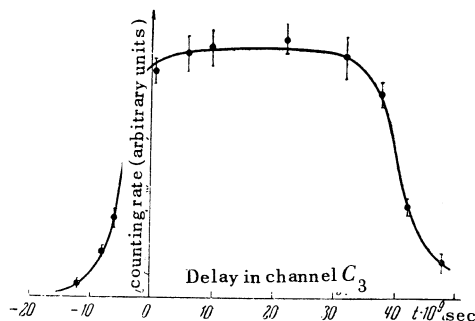


FIG. 3. Integral spectrum of K -meson decay time.

drawn in Fig. 3. It yields a mean lifetime of K -mesons of $(9.5 \pm 2.0) \times 10^{-9}$ sec, assuming a single-exponent decay. This result is in accord with Refs. 3-5.

¹ Balats, Lebedev and Obukhov, P.T.E. (in press).

² R. L. Garwin, Rev. Sci. Instr. **24**, 618 (1953).

³ L. Mezzetti and J. W. Keuffel, Phys. Rev. **95**, 858 (1954).

⁴ K. W. Robinson, Phys. Rev. **99**, 1606 (1955).

⁵ V. Fitch and R. Motley, Phys. Rev. **101**, 496 (1956).

Translated by C. R. Lubitz
109

A Method of Investigation of Radial-Phase Oscillations of Electrons in a Synchrotron

IU. M. ADO

*P. N. Lebedev Physical Institute
Academy of Sciences, USSR*

(Submitted to JETP editor June 8, 1956)

J. Exptl. Theoret. Phys. (U.S.S.R.) **31**, 533-534

(September, 1956)

IT is well known that in electron accelerators of synchrotron type, the accelerating electrons fill

ERRATA TO VOLUME 4

	reads	should read
P. 218, column 2, Eq. (10)	$\dots \xi^{(\sqrt{3}+2)} (2-\sqrt{3})$	$\dots \xi^{(\sqrt{2}+2)} / (2-\sqrt{3}) \dots$
P. 219, column 1, Eq. (11)	$\dots (t \xi) \sqrt{3/2} \dots$	$\dots (t \xi) \sqrt{3/2} \dots$
P. 219, column 1, Eq. (12)	$y^2 = \rho^{2/3}$	$y^2 - \rho^{2/3} \gg 1$
P. 223, column 1, Eq. (45)	$\dots (E_0 \mu^{3/4}) \sqrt{3/4}$	$\dots (E_0 \mu^{3/4}) \sqrt{3}/4$
P. 223, column 2, Eq. (46)	$\dots \mu^{3\sqrt{3/4}} \dots$	$\dots \mu^{3\sqrt{3/4}} \dots$
P. 225, column 1, 3 lines above Eq. (1.1)	transversality	cross section
P. 225, column 1, 3 lines above Eq. (1.2)	transversality	cross section
P. 256, column 1, Eq. (37)	$\dots \frac{55\sqrt{3}}{48} \dots$	$\dots \frac{55}{\sqrt{3} \cdot 48} \dots$
P. 289, column 2, Eq. (2)		$I = \sum_n \frac{1}{2n+1} A_n \sum_{\nu=-n}^n \frac{1}{1+i\omega\tau} Y_{n\nu}^{(n_1)} Y_{n\nu}(n_2)$
P. 377, column 1, last line	$\delta_{35} = \eta - 21 \times \eta^5$	$\delta_{35} - 21 \eta^5$
P. 436-7	Figures 2 and 3 should be exchanged.	
P. 449, column 1, last Eq.	$\dots Y_{lm} \varphi_{\sigma \alpha}$	$\dots Y_{lm} \varphi_{\sigma \alpha}$
P. 449, column 2, Eq. (12)	$\dots W(l, j, \sigma 1; j) \dots$	$\dots W(l, j, \sigma 1; \sigma j) \dots$
P. 451, column 1, Eq. (7)	$\dots D_{\alpha \beta}^{(1)}(p, 0, \lambda', \lambda) = \dots$	$\dots D_{\alpha \beta}^{(1)}(p, \omega_0, \lambda', \lambda) = \dots$
P. 541, column 1, Eq. (28)	$M_{++}^{* \text{monex}}$	$M_{+}^{* \text{monex}}$
P. 543, column 2, Eq. (35)	$\dots \int \rho^2 - \tau^2 + l_0^2$	$\dots \int \dots \rho^2 < \tau^2 + l_0^2$